Habitat-based density models of pack-ice seal distribution in the southern Weddell Sea, Antarctica

Oosthuizen WC, Reisinger RR, Bester MN, Steinhage D, Auel H, Flores H, Knust R, Ryan S, Bornemann H

SUPPLEMENTARY INFORMATION CONTENT

Supplement 9

Table S3. *Visual line transect survey density surface models (DSMs) for crabeater seals*
Table S4. *Visual line transect survey density surface models (DSMs) for Weddell seals*
Figures S16. *Crabeater seal model diagnostic plots*
Figures S17. *Weddell seal model diagnostic plots*

Supplement 10

Figure S18. *Change in model predicted pack ice seal abundance with different levels of availability*

Supplement 11

Figure S19. *Model predicted pack ice seal density plotted against relative abundance of prey species sampled in ecosystem surveys*

Supplement 12

Literature cited

Supplement 1

Text S1. *Validating strip transect detection assumptions*

The digital survey was based on strip transect sampling. To verify the assumption that all seals on the strip are detected and counted, we estimated the number of photographs predicted to contain seals with a closed-capture capture-recapture analysis. An encounter history matrix with three "encounters" was built, where encounter columns represented the three observers. For all images with detections, a '1' recorded that a specific observer detected the seal, whereas a '0' recorded that a specific observer detected no seals in a particular image. Observer-specific detection probability was subsequently estimated by fitting a closed-capture Huggins model in MARK 8.0 (White and Burnham 1999) with 'time' (i.e., observer) as an explanatory variable.

Observer-specific detection probability (p) on transect lines was $p_1 = 0.66$ (95 % confidence interval: 0.59 – 0.72), $p_2 = 0.86$ (0.80 – 0.90) and $p_3 = 0.98$ (0.94 – 0.99), respectively. The closed-capture Huggins model predicted that 185 (95 % confidence interval: 185 – 188) photographs contained seals. This result validates our "observed" data (we selected 185 images with seals) and the use of strip transect methods for the digital survey.

Supplement 2

Text S2. ***Haulout behaviour of pack ice seals and estimates of availability to sampling***

We used the time spent in and out of the water by satellite tagged crabeater and Weddell seals (Southwell 2005, Bengtson et al. 2011, Forcada et al. 2012) to correct on-ice abundance estimates. These studies showed that the probability of being hauled out consistently peaked around 0.7 in the hours on either side of local mid-day, when most of our surveys were conducted. Our main analysis thus assumed that 70 % of seals were available for detection during both the digital and visual surveys."

Forcada et al. (2012) conducted most of their surveys between 11:00 and 17:00 (thus one hour later in the afternoon than our surveys) and recorded a mean haul-out probability of 0.64 for crabeater seals and 0.65 for Weddell seals. Our slightly higher estimate is justified by not conducting surveys after 16:00 (when fewer seals are hauled out).

Southwell (2005) collected data on haulout behaviour of crabeater seals during the breeding season, which coincides with our digital survey. Southwell (2005) found *"a high, relatively constant proportion of seals were hauled out over a period of 6-7 h during daylight"* and that *"variation in haulout behaviour between seals was low"* (Figure S1).

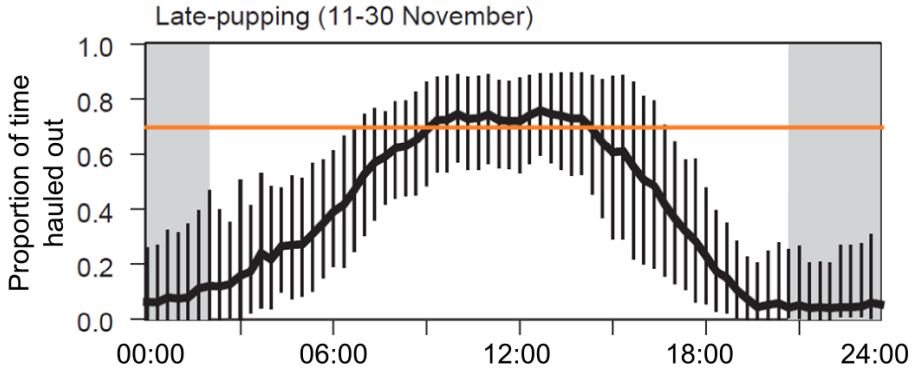

Figure S1. Haulout pattern of crabeater seals relative to local time (solar hour). The bold line is the mean proportion of days when a 20-minute period was recorded as 'dry' (hauled out); vertical lines indicate among-seal variation (± standard deviation). The orange horizontal line marks the 0.7 estimate used as an availability parameter in density surface models. Figure reproduced from Southwell (2005).

Bengtson et al. (2011) also found that haul-out probability of crabeater seals peaked around mid-day (local solar time) through December to March (Figure S2).

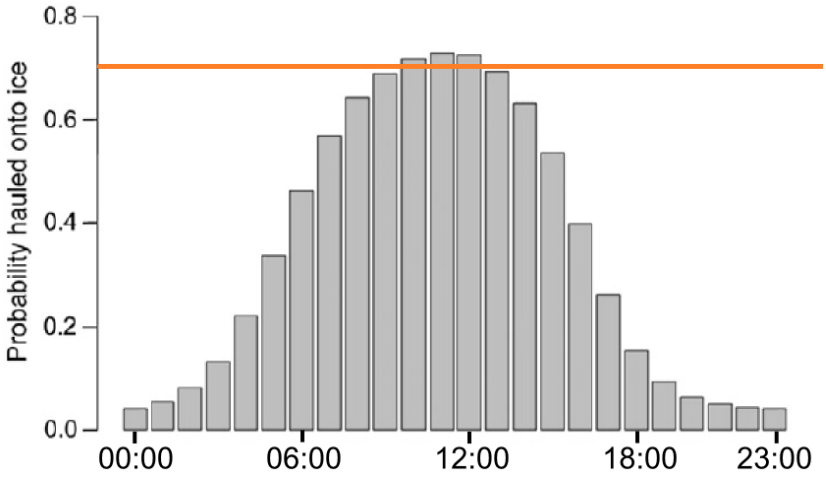

Figure S2. Haulout pattern of crabeater seals relative to local time (solar hour). The orange horizontal line marks the 0.7 estimate used as an availability parameter in density surface models. Figure reproduced from Bengtson et al. (2011).

There is, however, individual variation in availability (e.g., due to different haulout behaviour of breeding and nonbreeding seals; Southwell 2005). Gurarie et al. (2017) used the crabeater seal haulout probabilities from Bengtson et al. (2011) to adjust their crabeater seal abundance estimates. Gurarie et al. (2017)'s figure (Figure S3) indicate a broad peak in haulout probabilities around mid-day of approximately 80 % in November, which decreased to 70 – 75 % in January February, and to 60 % in March. For Weddell seals, Gurarie et al. (2017) presented hourly haul-out percentages for seals instrumented at Drescher Inlet in January-March. These data also indicated low variation in haulout behaviour and haulout probabilities of near 70 % in the hours before and after solar mid-day (Figure S4).

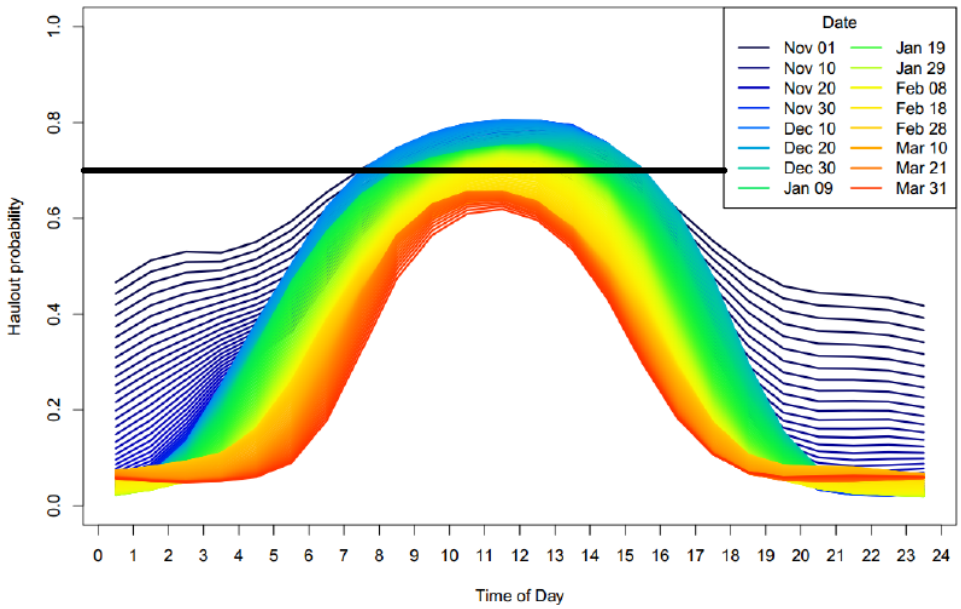

Figure S3. Crabeater seal haulout probabilities from November to March. The black horizontal line marks the 0.7 estimate used as an availability parameter in density surface models. Figure reproduced from Gurarie et al. (2017).

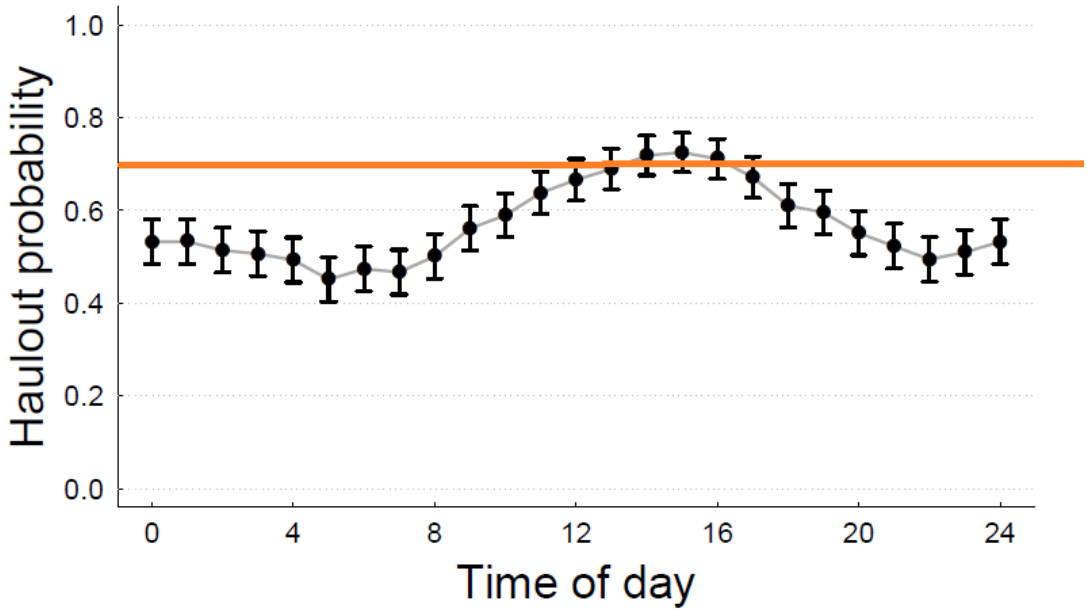

Figure S4. Weddell seal haulout probabilities from January to March. The orange horizontal line marks the 0.7 estimate used as an availability parameter in density surface models. Figure reproduced from Gurarie et al. (2017).

Supplement 3

Text S3. *Extrapolation assessment with "dsmextra"*

Habitat models allow animal densities to be extrapolated from sampled to unsampled locations (e.g., Mannocci et al. 2015, Derville et al. 2018, Purdon et al. 2020, Wege et al. 2020). However, extrapolations to conditions outside the range of those encountered in the surveyed area can easily lead to unreasonable results. Several factors influence the reliability of predictions in unsampled areas, including the environmental similarity between locations where data were collected and those where predictions are made (Conn et al. 2015, Bouchet et al. 2020, Sequeira et al. 2018).

We limited predictions of pack ice seal densities to areas of multivariate environmental space (*cf.* geographic extrapolation) that was informed by reference (survey) data. We used the package "dsmextra" (Bouchet et al. 2019) in R 3.6.3 (R Core Team 2020) to quantify and visualise extrapolation in environmental space, and to set boundaries of prediction areas. We limited our prediction area to cells where environmental conditions were within the sampled range of the covariate data and avoided both univariate and combinatorial extrapolation. Additionally, the percentage of data nearby (%N) was used as a quantitative measure of the proportion of reference data lying within the 'neighbourhood' of any prediction cell. We focus our DSM inference on areas that were informed by at least 10 % reference data (%N > 10 %) in the neighbourhood of prediction cells (Bouchet et al. 2020). Full methodological details regarding extrapolation analyses are given in Bouchet et al. (2020). Examples of other marine mammal studies that mapped extrapolations in environmental space in the context of habitat-based density surface models include Mannocci et al. (2015) and García-Barón et al. (2019).

Extrapolation assessment of digital strip transect survey

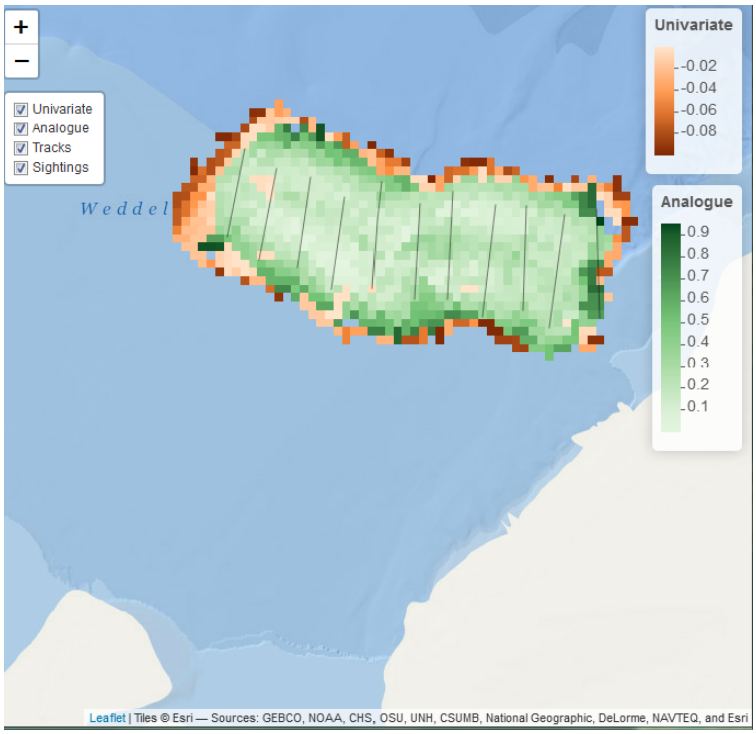

Figure S5. Map showing extrapolation (ExDet) values and transect lines. The prediction grid used for the digital strip transect survey density surface models was limited to analogue conditions, i.e. the green shading on this figure. The prediction grid excluded areas where univariate (orange shading on figure) or combinatorial extrapolation was required.

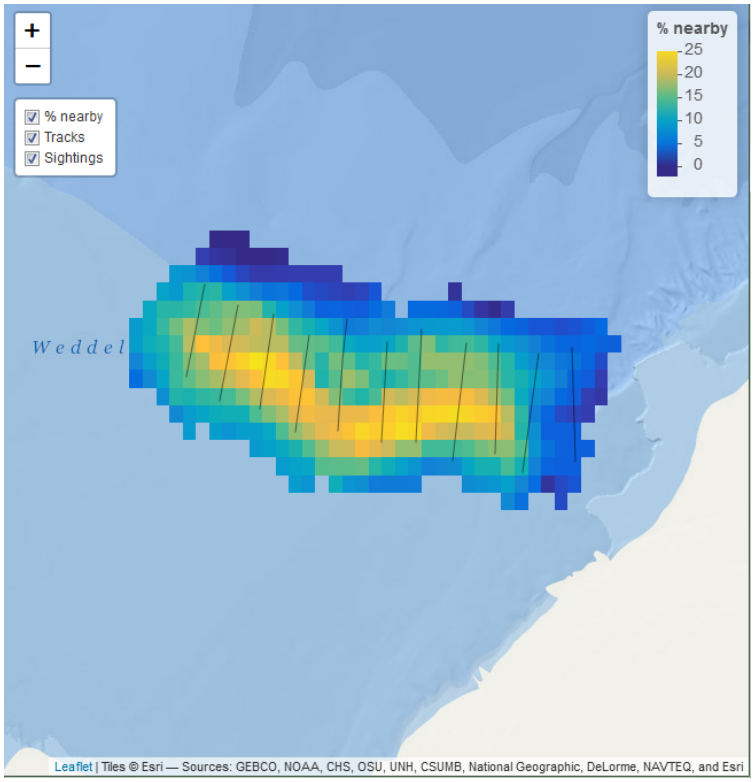

Figure S6. Map showing proportion of data nearby (%N) and transect lines for the digital strip transect survey. We focus our DSM inference on areas that were informed by at least 10 % reference data (%N > 10 %) in the neighbourhood of prediction cells. Predictions in areas where %N was less than 10 % but more than zero (%N > 0 %) are more speculative (cross-hatched in figures presented in the main text).

Extrapolation assessment of visual line transect survey

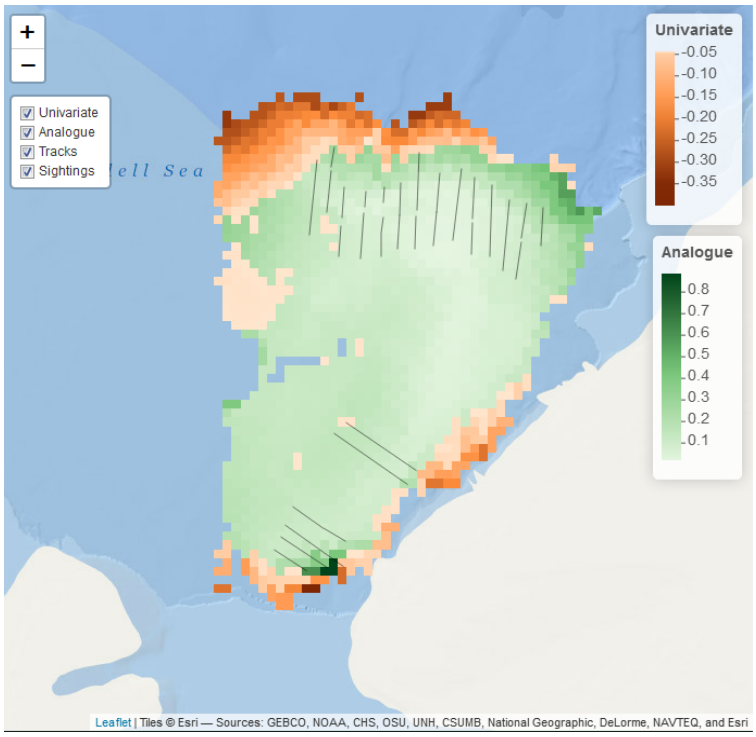

Figure S7. Map showing extrapolation (ExDet) values and transect lines. The prediction grid used for the visual line transect survey density surface models was limited to analogue conditions, i.e. the green shading on this figure. The prediction grid excluded areas where univariate (orange shading on figure) or combinatorial extrapolation was required.

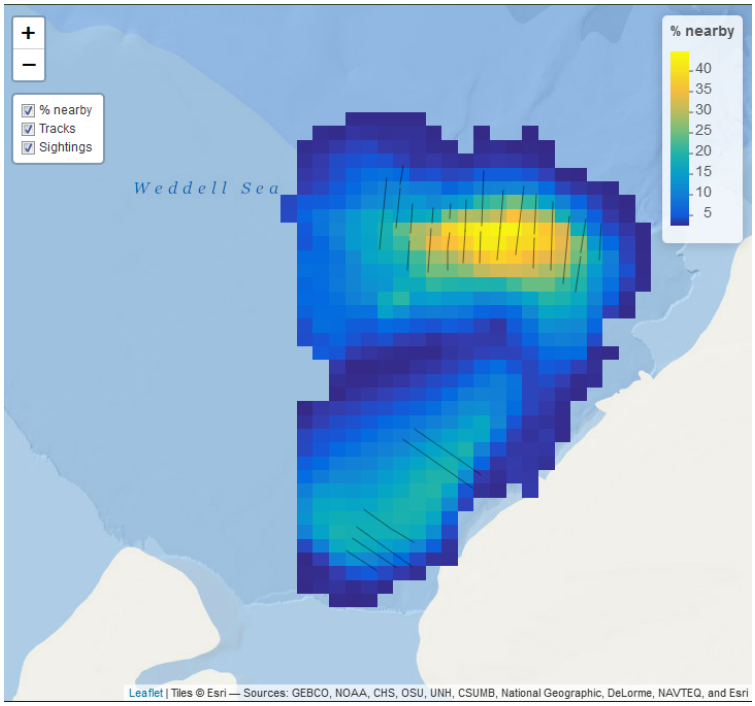

Figure S8. Map showing proportion of data nearby (%N) and transect lines for the visual line transect survey. We focus our DSM inference on areas that were informed by at least 10 % reference data (%N > 10 %) in the neighbourhood of prediction cells. Predictions in areas where %N was less than 10 % but more than zero (%N > 0 %) are more speculative (cross-hatched in figures presented in the main text).

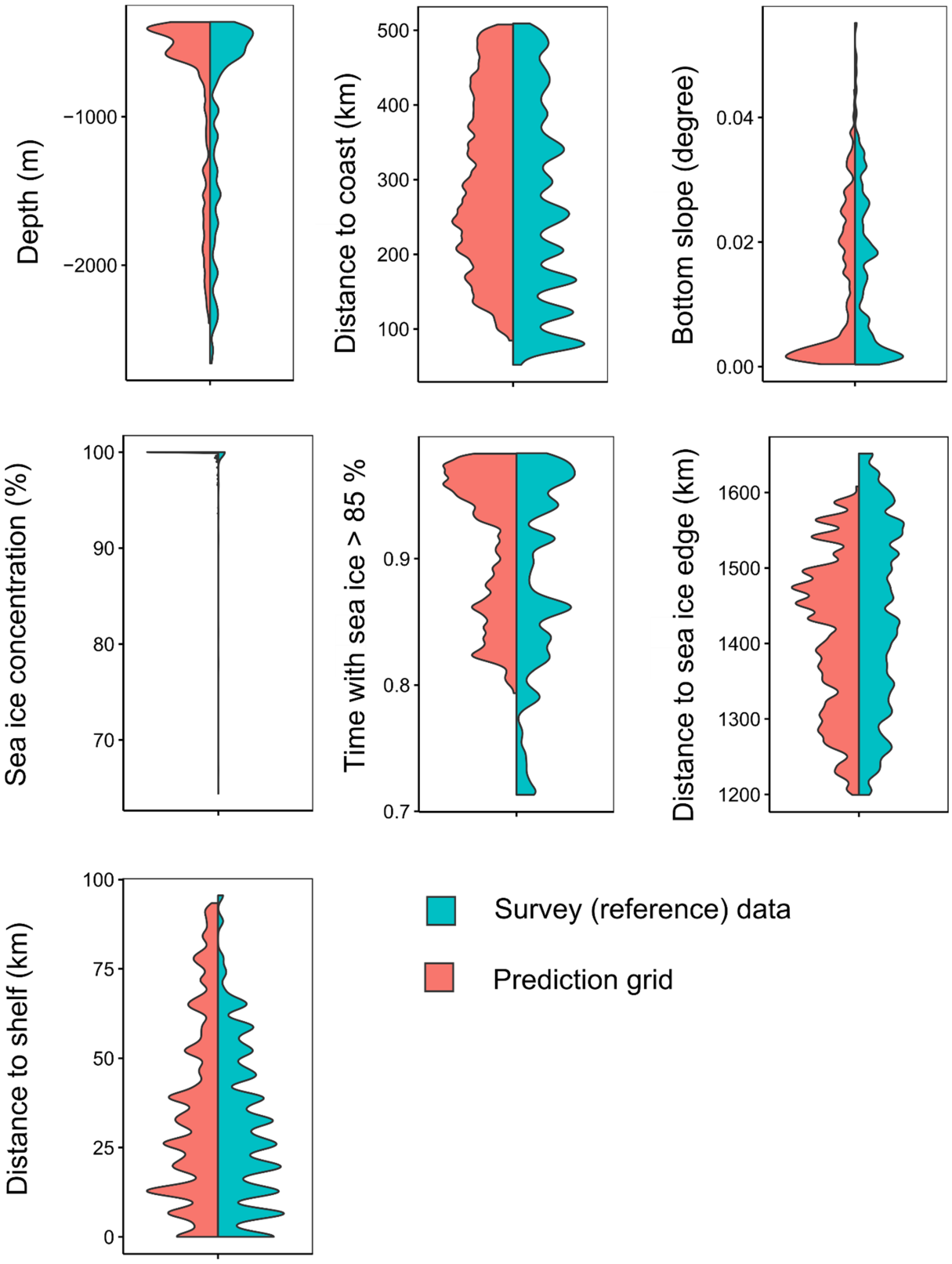

Figure S9. Density distributions (bandwidth adjustment = 0.2) of environmental covariates along grid cells covered by transects of the digital strip transect survey, and within the main prediction area (%N > 10 %).

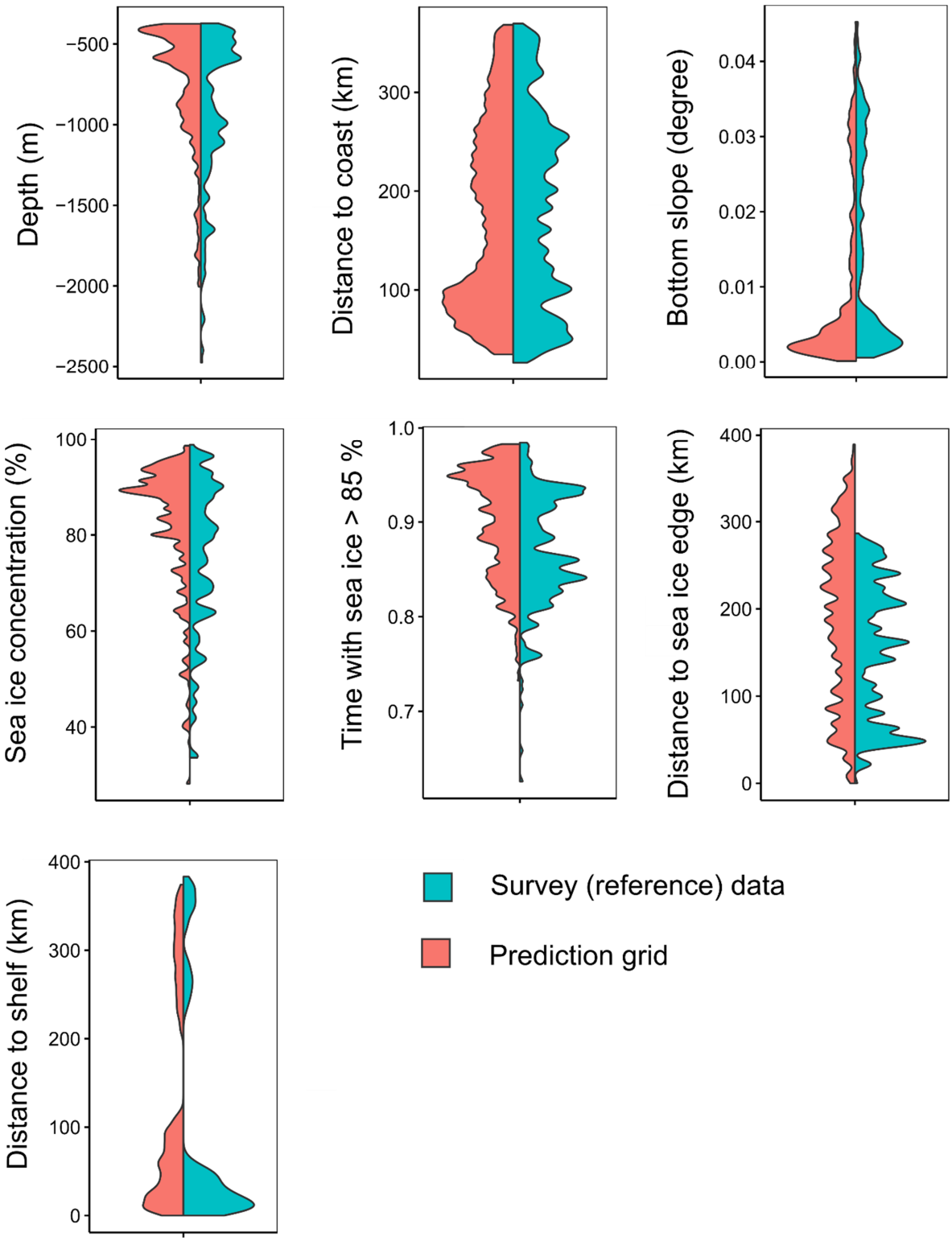

Figure S10. Density distributions (bandwidth adjustment = 0.2) of environmental covariates along grid cells covered by transects of the visual line transect survey, and within the main prediction area (%N > 10 %).

Supplement 4

Text S4. ***Environmental covariates used in density surface models of pack ice seals in the southern Weddell Sea***

Depth (m)

Source: General Bathymetric Chart of the Oceans (British Oceanographic Data Centre) http://www.gebco.net at a resolution of 0.125°.

Depth is important for benthic vs. pelagic foraging in marine predators, and indicates whether locations are on the continental shelf (typically depths of 300 m to 500 m) or off the continental shelf (e.g., depths beyond 1000 m).

Bottom slope (°)

Source: Derived from General Bathymetric Chart of the Oceans bathymetry data using the raster::terrain function in R (with opt = "slope").

Higher turbulence and upwelling of Circumpolar Deep Water (or Warm Deep Water) along steep continental slopes can increase local marine productivity.

Distance to continental shelf break (km)

Source: Derived from General Bathymetric Chart of the Oceans bathymetry data. We calculated distance (using function raster::distance) to the 1000 m isobath at the continental shelf edge, and excluded the 1000 m isobath in the southern Filchner Trough from this derivation.

Upwelling of nutrient-rich Warm Deep Water along the continental shelf break slopes and across-shelf transport of Warm Deep Water by the Antarctic Slope Front may increase local biological productivity in the vicinity of the continental shelf break.

Distance to coast (km)

Source: Derived from General Bathymetric Chart of the Oceans bathymetry data. We calculated distance (using function raster::distance) the nearest 0 m (sea level) isobath.

Weddell seals often haul out on coastal fast-ice, and may preferentially forage near these haulouts.

Sea ice concentration (%)

Source: NSIDC concentration data, processed by the SMMR/SSMI NASA Team (http://nsidc.org/data/docs/daac/nsidc0051_gsfc_seaice.gd.html). Sea ice concentration data (resolution 12.5 km) were obtained for every day that surveys took place. We matched the segment survey dates to the nearest daily data, and calculated the average sea ice concentration

Sea ice is a critical habitat for pack ice seals. The physical characteristics and extent of the sea ice (e.g., coastal fast ice, interior pack ice, marginal ice zone, etc.) are important variables structuring pack ice seal distribution.

Distance to ice edge (km)

Source: NSIDC concentration data derivative. To calculate distance to the sea ice edge, we first calculate a contour line for 15% sea ice concentration (using function raster::rasterToContour in R) and we then calculate, for each pixel, the distance to the nearest position along the contour line using function raster::distance. Visual inspection of the daily sea ice concentration data showed that spurious sea ice edges due to very small, isolated sea ice or open water features (but not included true polynyas) were not present in our case. In January 2014, the nearest distance to the ice edge probably started out as a large polynya, which opened into open water to the north in February.

The ice edge (including polynya ice edges) is an important foraging habitat for marine predators, including some pack ice seal species (e.g., Gurarie et al. 2017, Michelot et al. 2020).

Proportion of time the ocean is covered by sea ice of concentration 85 % or higher ("multiyear sea ice cover") (%)

Source: AMSR-E satellite estimates of daily sea ice concentration at 6.25 km resolution. Concentration data from 1-Jan-2003 to 31-Dec-2010 was used to calculate sea ice cover consistency over multiple years. The fraction of time each pixel was covered by sea ice of at least 85% concentration was calculated for each pixel in the original (Polar stereographic) grid. The data was subsequently regridded to 0.1-degree grid using triangle-based linear interpolation. Data obtained from https://data.aad.gov.au/metadata/records/Polar_Environmental_Data.

(Maps of environmental covariates appear on following pages)

Digital strip transect survey (November 2013)

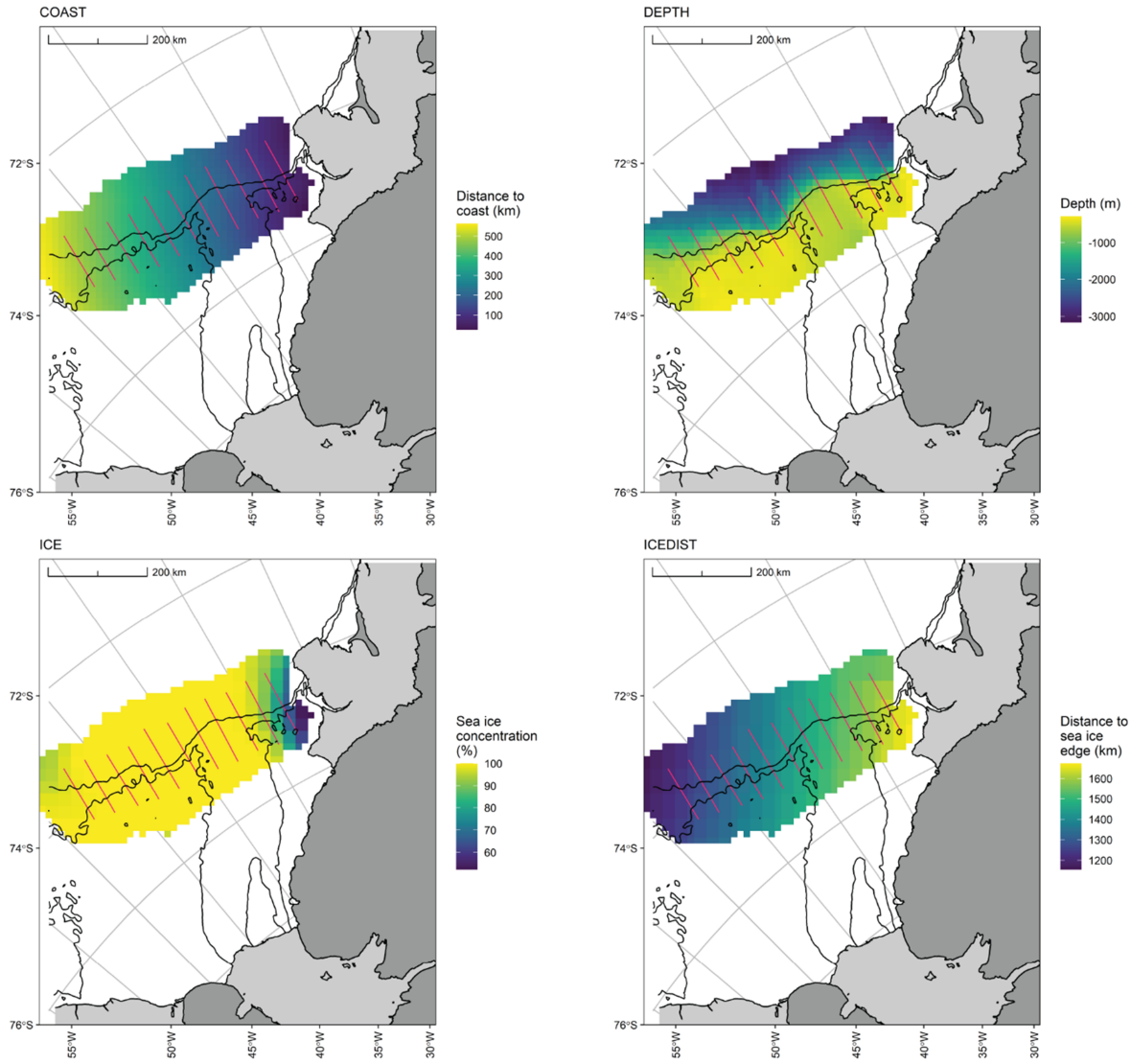

Figure S11. Environmental variables used as covariates in density surface models of digital strip transect data. Distance to the coast (COAST) is given as distance (km) to the nearest coastline; depth (DEPTH) is the ocean depth (m) derived from bathymetry data; sea ice concentration (ICE) is satellite derived sea ice concentration given in %; distance to the ice edge (ICEDIST) is the distance (km) to the nearest 15 % ice concentration contour line (the daily 15 % contour lines are shown, in blue, on the maps of the January and February 2014 visual transect surveys, but were outside the boundary of the maps in the November 2013 digital surveys.

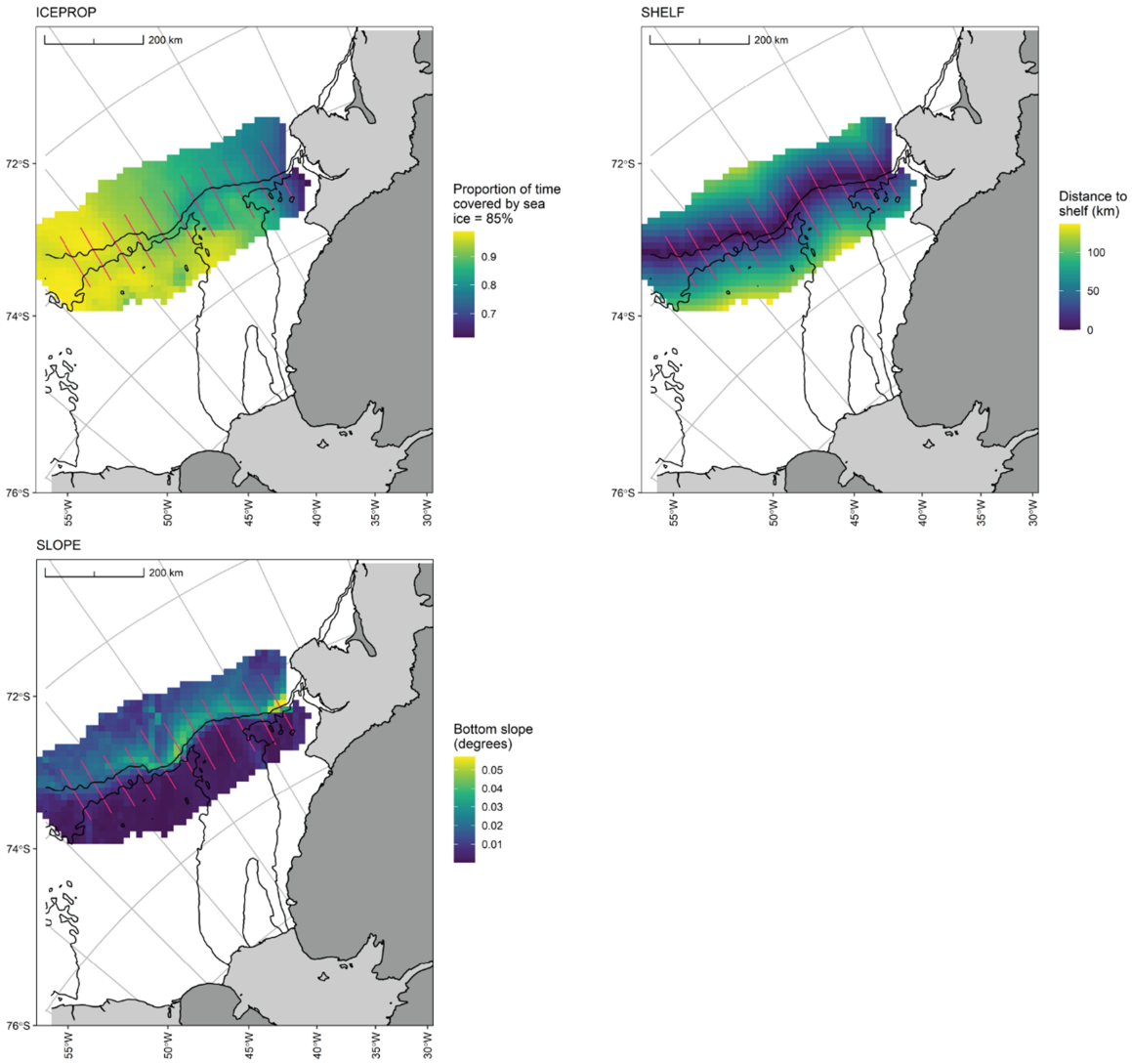

Figure S11 (continued). ICEPROP is the proportion of time (%) that the ocean is covered by sea ice of concentration 85 % or higher ("multiyear sea ice cover"); the distance (km) to the continental ice shelf (SHELF) was derived as the distance to the 1,000 m bathymetric contour; SLOPE is the gradient of the ocean floor slope (in degrees) as derived from bathymetry data.

Visual line transect survey (January to February 2014)

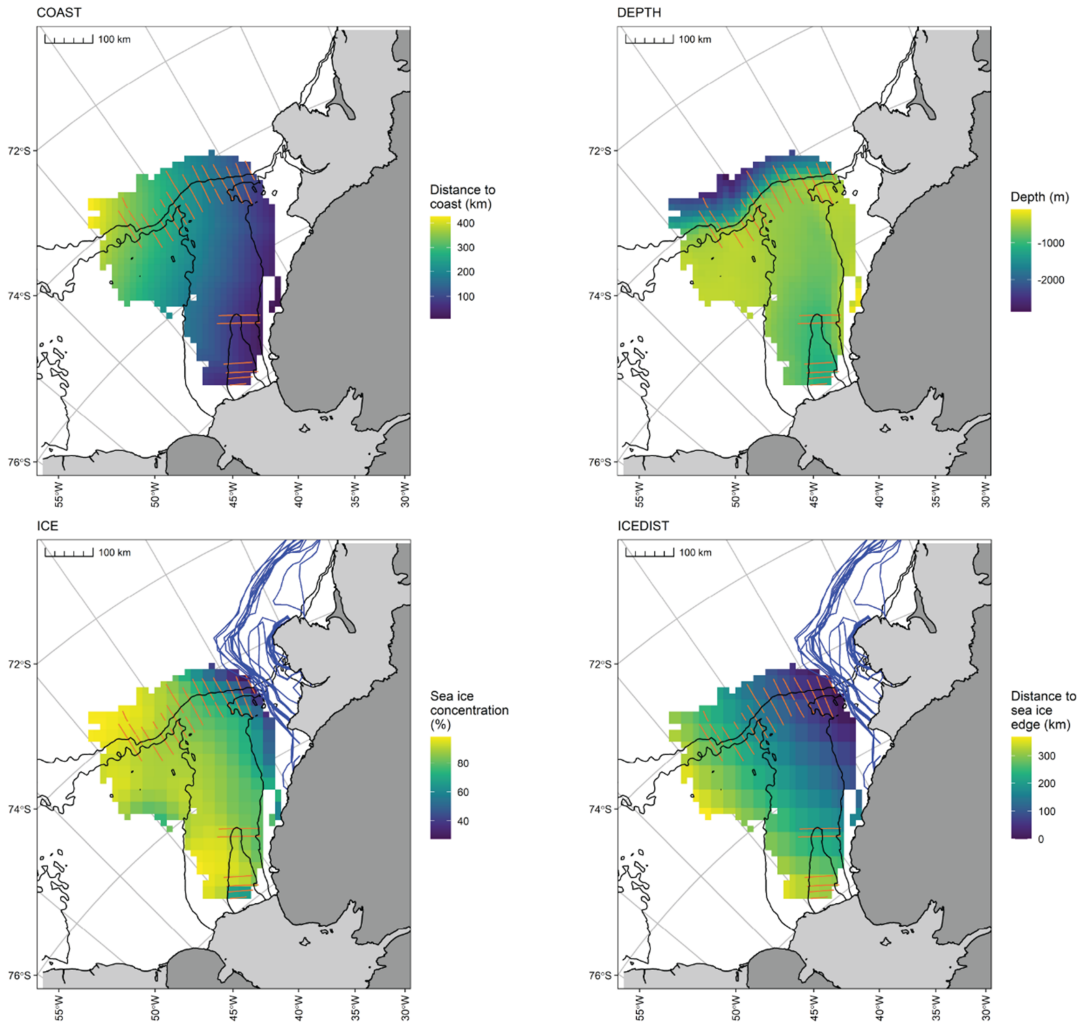

Figure S12. Environmental variables used as covariates in density surface models of visual line transect data. Distance to the coast (COAST) is given as distance (km) to the nearest coastline; depth (DEPTH) is the ocean depth (m) derived from bathymetry data; sea ice concentration (ICE) is satellite derived sea ice concentration given in %; distance to the ice edge (ICEDIST) is the distance (km) to the nearest 15 % ice concentration contour line. The 15 % contour lines of ice concentration for each survey date are shown in blue on the ICE and ICEDIST maps.

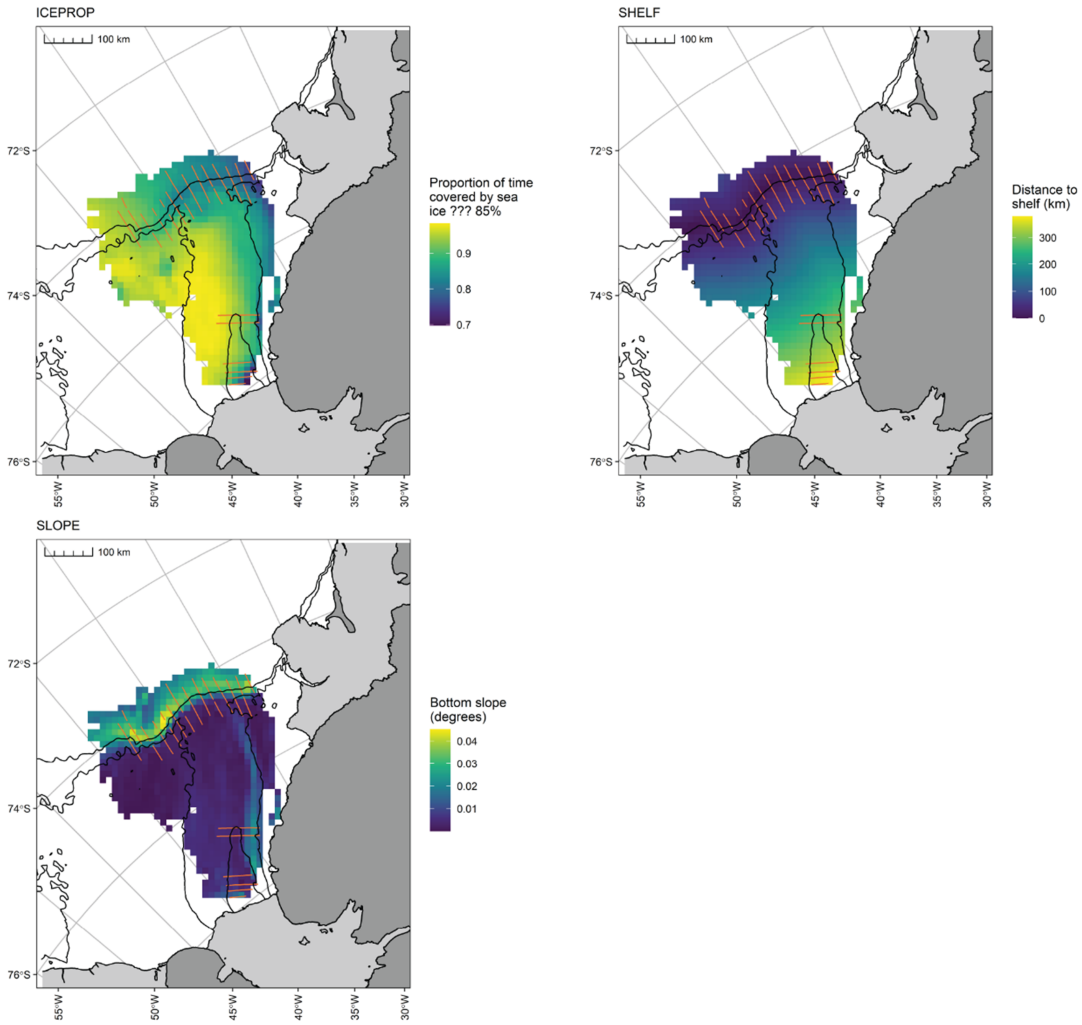

Figure S12 (continued). ICEPROP is the proportion of time (%) that the ocean is covered by sea ice of concentration 85 % or higher ("multiyear sea ice cover"); the distance (km) to the continental ice shelf (SHELF) was derived as the distance to the 1,000 m bathymetric contour; SLOPE is the gradient of the ocean floor slope (in degrees) as derived from bathymetry data.

Supplement 5

Text S5. *Ecosystem surveys in the southern Weddell Sea (January to February 2014)*

Macrozooplankton survey

Macrozooplankton was sampled with a Multiple opening Rectangular Midwater Trawl (M-RMT). We used data from 22 stations (sampled from 2 January 2014 to 11 February 2014) where depth-stratified hauls were collected from a depth of 200 m to the surface. The krill species *Euphausia superba*, *Euphausia crystallorophias* and *Thysanoessa macrura* were identified from catches. We used the density of *E. superba* and *E. crystallorophias* (abundance per volume filtered), expressed as individuals m^{-3}, as an index of macrozooplankton abundance.

Fish survey

Pleuragramma antarctica and *Trematomus* spp. were obtained from 21 scientific bottom trawls made between 3 January 2014 and 12 February 2014 at water depths between 214 m and 1,750 m. Fish biomass data were recorded per species immediately after each trawl. We used the total biomass (g) per catch, standardized to an area of 1,000 m^2, as a measure of fish abundance.

Additional information is available in Knust and Schröder (2014).

Supplement 6

Table S1. ***Digital strip transect survey density surface models (DSMs) and model diagnostics***

Table S1. Density surface models fitted to digital strip transect survey data collected in the Weddell Sea, Antarctica, in November 2013. All combinations of "uncorrelated" (Spearman $|r| < |0.7|$) covariates were fitted as models. Abundance ($\widehat{N}$) was predicted to a prediction grid (57,031 km^2) that did not require univariate or combinatorial extrapolation and that had at least 10 % (%N ≥ 10 %) reference data nearby.

Response distribution[1]	Model smooth terms[2]	AIC	REML	Deviance explained (%)	$\widehat{N}$	$\widehat{N}$ (95% CI)
tw (p=1.12)	s(ice concentration) s(time with ice ≥85%) s(depth) s(distance to shelf break)	519.2	258.8	24.79	39,939	33,582 - 47,500
tw (p=1.12)	s(ice concentration) s(time with ice ≥85%) s(slope)	522.6	259.9	23.12	40,840	34,322 - 48,596
tw (p=1.12)	s(ice concentration) s(distance to ice) s(depth) s(distance to shelf break)	524.9	260.4	22.57	39,614	33,057 - 47,472
tw (p=1.12)	s(ice concentration) s(distance to coast) s(depth) s(distance to shelf break)	525.9	260.9	22.17	39,752	33,142 - 47,680
tw (p=1.12)	s(ice concentration) s(distance to ice) s(slope)	527.9	261.5	19.32	38,444	32,340 - 45,702
tw (p=1.13)	s(ice concentration) s(distance to coast) s(slope)	529.0	262.0	18.81	38,922	32,716 - 46,305

[1.] Response distribution: tw = Tweedie. The same set of models were fitted with a negative binomial response distribution, but these models had higher AIC values and poorer model diagnostics.

[2.] Model smooth terms: ice concentration = sea ice concentration, time with ice ≥85% = the fraction of time the ocean is covered by sea ice of concentration 85 % or higher ("multiyear

sea ice cover"), depth = depth, distance to shelf break = distance to continental shelf break, slope = bottom slope, distance to ice = distance to sea ice edge, distance to coast = distance to nearest coast.

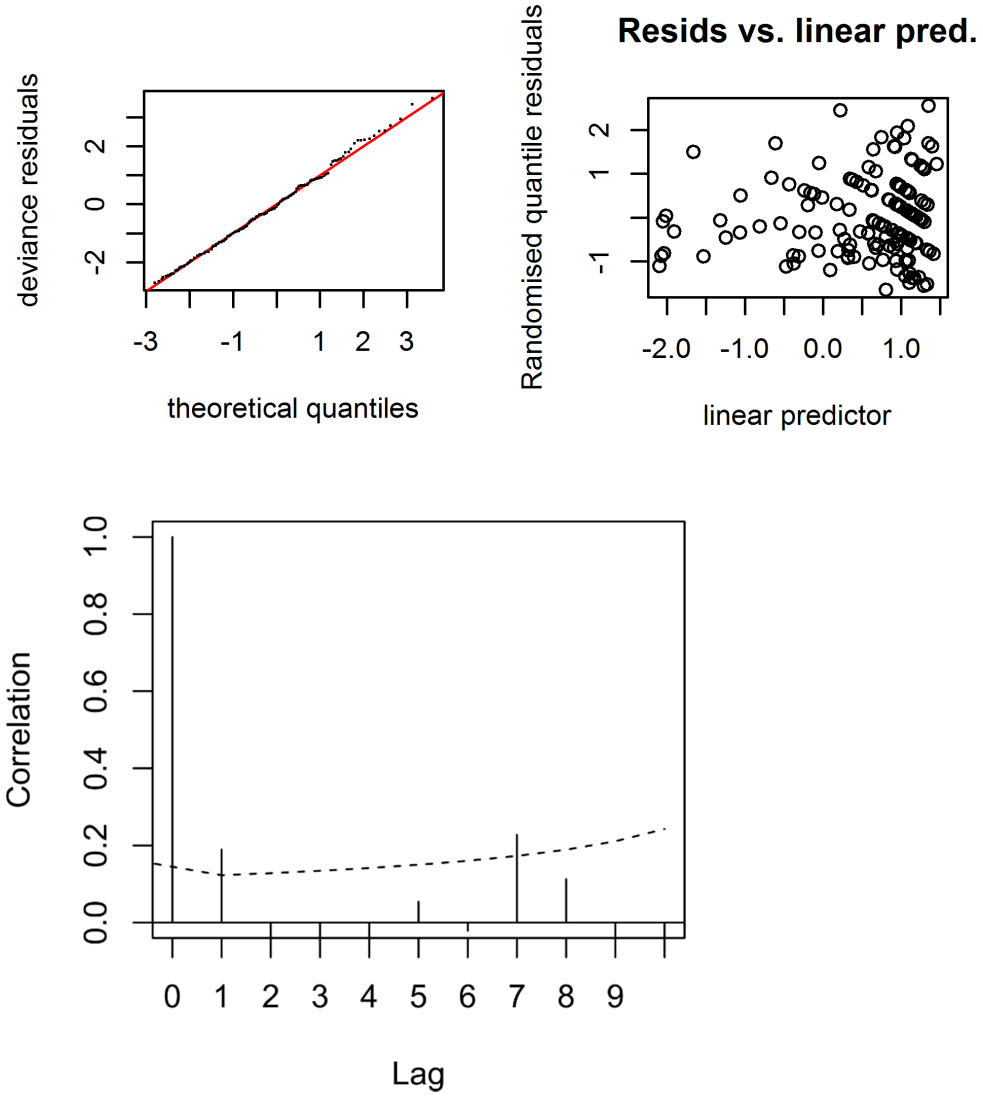

Figure S13. Normal Q–Q plot, randomised quantile residuals versus linear predictor plot, and correlogram for the digital strip transect survey density surface model with the lowest AIC (Table S1). The correlogram showed weak autocorrelation (r = 0.19 at a lag of 1 segment) in the model residuals.

Supplement 7

Figure S14. ***Digital strip transect survey imagery***

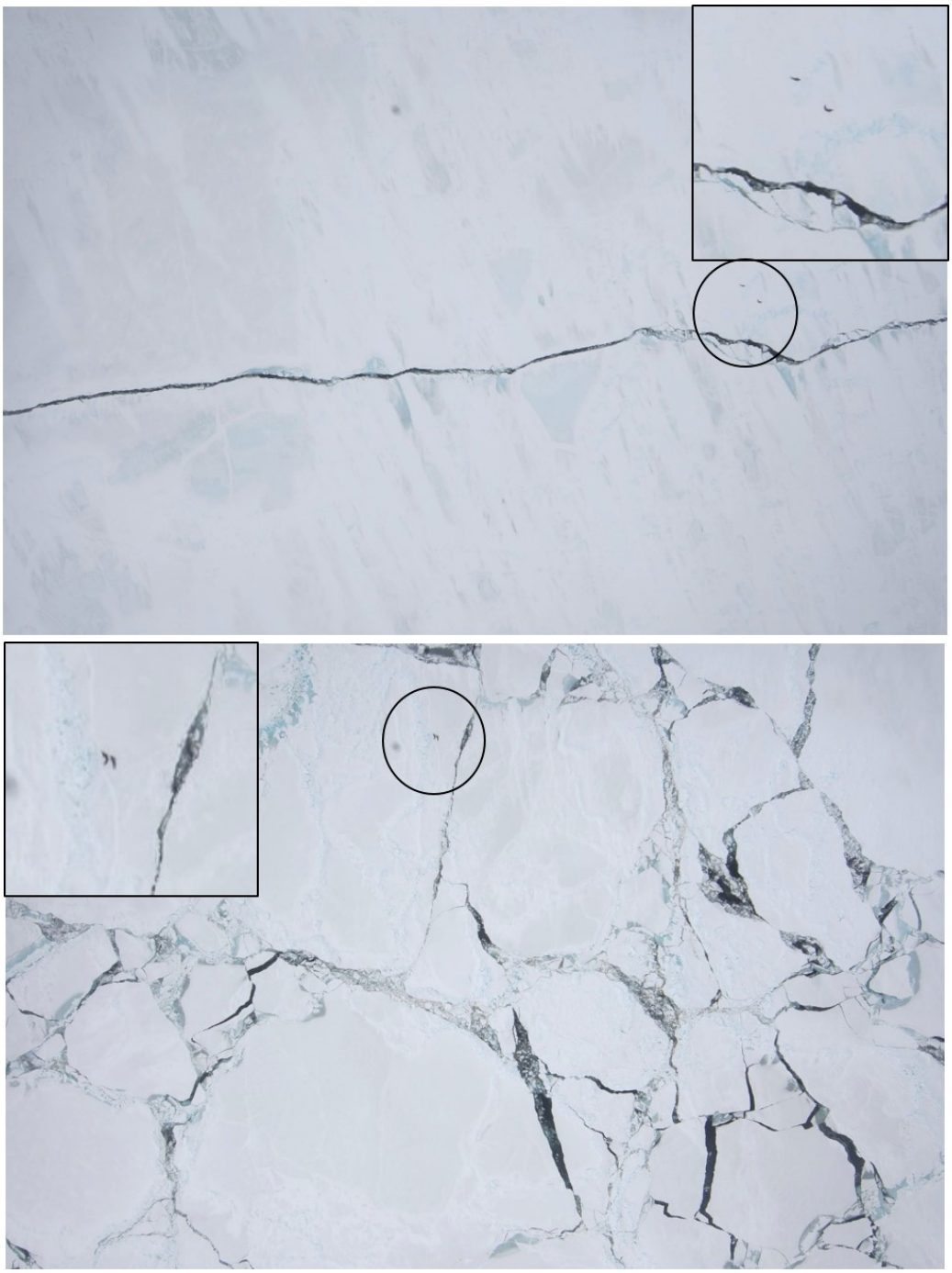

Figure S14. Two high-resolution images from the digital strip transect survey showing typical sea ice conditions in the southern Weddell Sea during November 2013. Inset: seals hauled out on ice (magnified view of encircled area).

Supplement 8

Text S6. *Detection function modelling*

Distance sampling methods assume detectability is primarily related to the distance between objects and the observer. The detection probability is modelled as a function of the perpendicular distance, under the assumption that all objects within the immediate vicinity of the track line are detected (i.e., g(0) = 1)) (Burt et al. 2014). We assumed that g(0) equalled unity and consider this assumption plausible given that seal densities were relatively low and taking the experience level of the observers into account.

The detection function in the visual line transect survey was characterized by a wide shoulder (Figure S11). The most parsimonious model (Table S2) contained a hazard-rate key function and observer as a covariate. Average detection probability was 0.57 (CV = 0.04) and a Chi-square goodness of fit test showed that the detection function fitted the data well (χ_1^2 = 0.02, p = 0.88). Failure to adopt distance sampling methodology would therefore have underestimated seal densities by an average of 1.78 times in each surveyed segment.

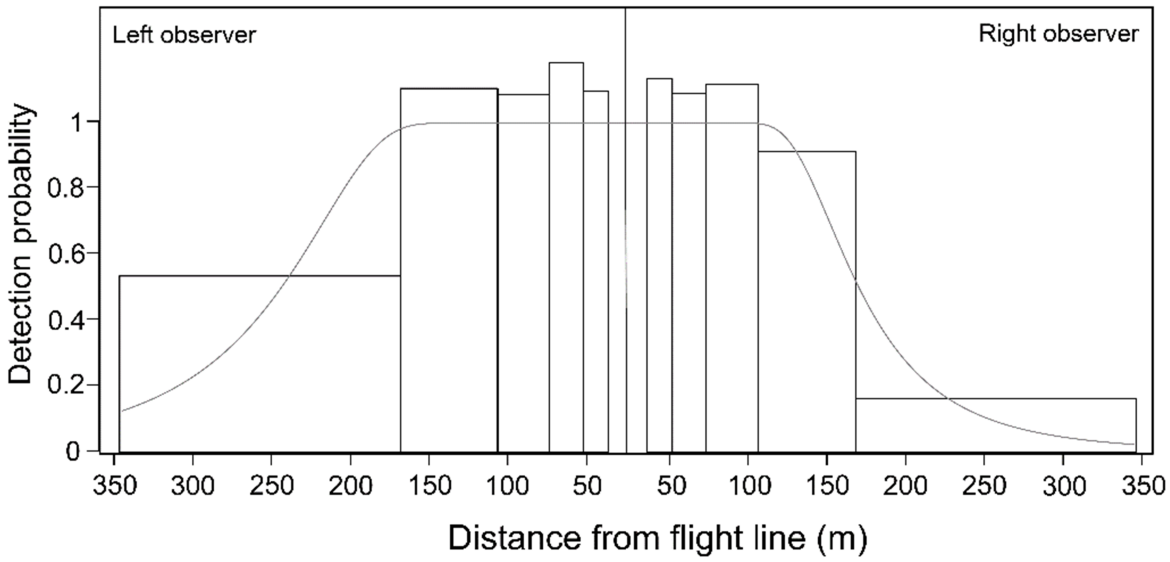

Figure S15. Detection probabilities for the visual line transect survey. Observers on the left and right side of the aircraft had different detection functions.

Table S2. *Detection function modelling*

Table S2. Detection function model selection results. Half-normal (hn) and hazard-rate (hr) detection functions were fitted via maximum likelihood to describe the decrease in detection probability with distance from the line. Observer, group size (range 1 to 6, fitted as a factor with two levels (1, ≥ 2) or as a continuous covariate), seal species, mean visibility and ice structure were included as covariates. The model in bold font was selected. The model hr + Ice structure had zero degrees of freedom in the Chi-square goodness of fit test and was therefore not considered as a plausible model. No covariates were considered where model key functions were paired with cosine adjustment terms. np is the number of parameters. ΔAIC is the difference in AIC between the model with the lowest AIC value and the relevant model.

Model key function	Covariate	np	Δ AIC	Average detection (p)	SE (p)
hr	**Observer**	**3**	**0.00**	**0.57**	**0.02**
hn	Observer + size (factor)	3	3.85	0.45	0.02
hn	Observer + size (linear)	3	5.13	0.45	0.02
hn	Observer	2	6.22	0.45	0.02
hn	Observer + species	3	7.34	0.45	0.02
hn	Observer + visibility	3	7.92	0.45	0.02
hr	Size (factor)	3	32.50	0.55	0.03
hr	Species	3	33.87	0.57	0.03
hr	Size (linear)	3	33.99	0.56	0.03
hr	Intercept	2	34.22	0.56	0.03
hr (Cosine)	Intercept	2	34.22	0.56	0.03
hn (Cosine)	Intercept	2	34.97	0.54	0.06
hr	Visibility	3	36.19	0.56	0.03
hn	Size (factor)	2	35.69	0.47	0.02
hn	Size (linear)	2	36.80	0.47	0.02
hn	Species	2	36.94	0.47	0.02
hn	Intercept	1	37.23	0.47	0.02
hn	Visibility	2	39.19	0.47	0.02
hn	Ice structure	3	41.08	0.47	0.02

Supplement 9

Visual line transect survey density surface models (DSMs) and model diagnostics

Table S3. Density surface models fitted to visual line transect survey observations of crabeater seals collected in the Weddell Sea, Antarctica, in January and February 2014. All combinations of "uncorrelated" (Spearman |r| < |0.7|) covariates were fitted as models. Abundance ($\widehat{N}$) was predicted to a prediction grid (65,625 km^2) that did not require univariate or combinatorial extrapolation and that had at least 10 % (%N ≥ 10 %) reference data nearby.

Response distribution[1]	Model smooth terms[2]	AIC	REML	Deviance explained (%)	$\widehat{N}$	$\widehat{N}$ (95% CI)
Crabeater seals						
tw (p=1.18)	s(depth) s(slope) s(distance to shelf break) s(distance to coast) s(time with ice ≥85%)	1240.9	624.2	44.87	72,323	60,682 – 86,196
tw (p=1.19)	s(depth) s(slope) s(distance to shelf break) s(distance to coast) s(ice concentration)	1249.6	623.3	42.30	79,032	66,021 – 94,607
tw (p=1.20)	s(depth) s(slope) s(distance to shelf break) s(distance to coast) s(ice concentration)	1250.5	626.6	41.86	78,786	65,750 – 94,407

[1.] Response distribution: tw = Tweedie. The same set of models were fitted with a negative binomial response distribution, but these models had higher AIC values and poorer model diagnostics.

[2.] Model smooth terms: ice concentration = sea ice concentration, time with ice ≥85% = the fraction of time the ocean is covered by sea ice of concentration 85 % or higher ("multiyear sea ice cover"), depth = depth, distance to shelf break = distance to continental shelf break, slope = bottom slope, distance to ice = distance to sea ice edge, distance to coast = distance to nearest coast.

Table S4. Density surface models fitted to visual line transect survey observations of Weddell seals collected in the Weddell Sea, Antarctica, in January and February 2014. All combinations of "uncorrelated" (Spearman |r| < |0.7|) covariates were fitted as models. Abundance ($\widehat{N}$) was predicted to a prediction grid (65,625 km^2) that did not require univariate or combinatorial extrapolation and that had at least 10 % (%N ≥ 10 %) reference data nearby.

Response distribution[1]	**Model smooth terms**[2]	**AIC**	**REML**	**Deviance explained (%)**	$\widehat{N}$	$\widehat{N}$ **(95% CI)**
Weddell seals						
tw (p=1.12)	s(depth) s(slope) s(distance to shelf break) s(distance to coast) s(time with ice ≥85%)	727.6	368.0	18.70	29,538	23,143 - 37,701
tw (p=1.12)	s(depth) s(slope) s(distance to shelf break) s(distance to coast) s(ice concentration)	731.0	368.1	18.04	31,346	23,593 - 41,646
tw (p=1.15)	s(depth) s(slope) s(distance to shelf break) s(distance to coast) s(ice concentration)	746.2	373.7	11.81	30,087	23,483 - 38,549

[1.] Response distribution: tw = Tweedie. The same set of models were fitted with a negative binomial response distribution, but these models had higher AIC values and poorer model diagnostics.

[2.] Model smooth terms: ice concentration = sea ice concentration, time with ice ≥85% = the fraction of time the ocean is covered by sea ice of concentration 85 % or higher ("multiyear sea ice cover"), depth = depth, distance to shelf break = distance to continental shelf break, slope = bottom slope, distance to ice = distance to sea ice edge, distance to coast = distance to nearest coast.

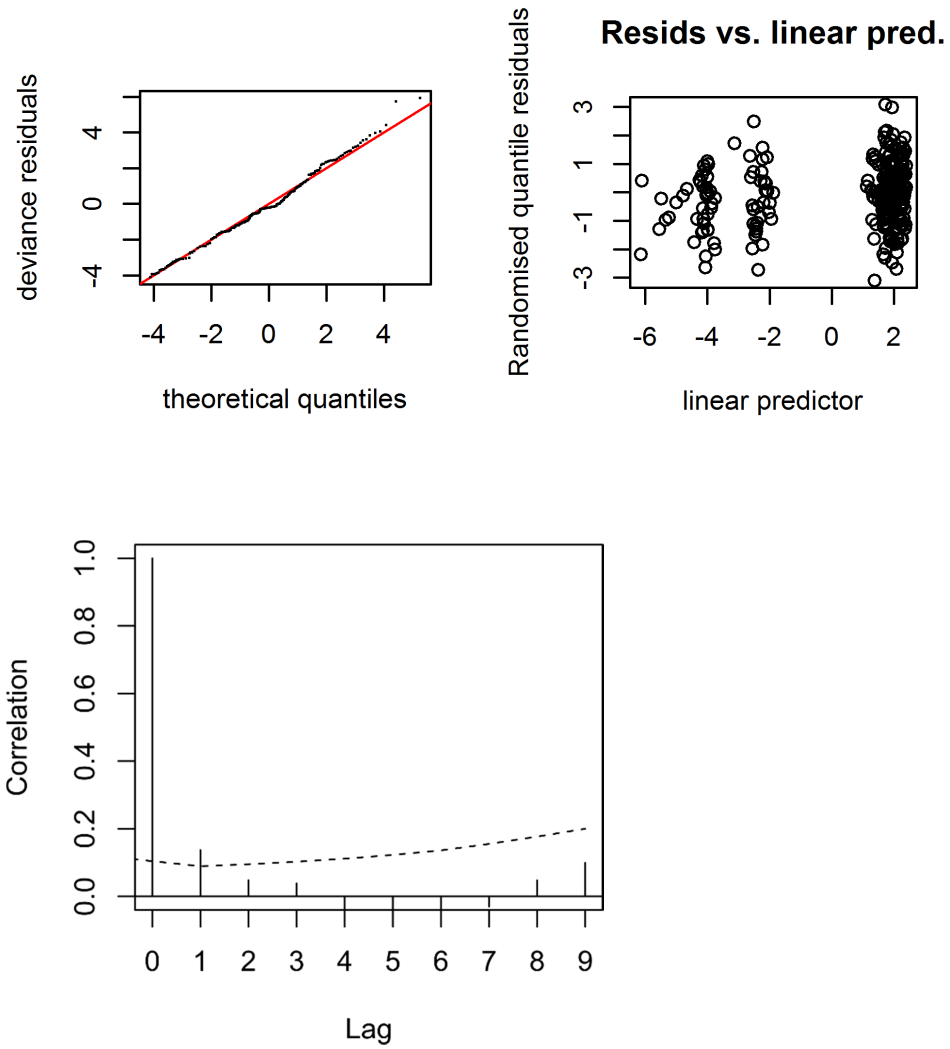

Figure S16. Normal Q–Q plot, randomised quantile residuals versus linear predictor plot, and correlogram for the crabeater seal density surface model with the lowest AIC (Table S8.1). The correlogram showed weak autocorrelation (r = 0.17 at a lag of 1 segment) in the model residuals.

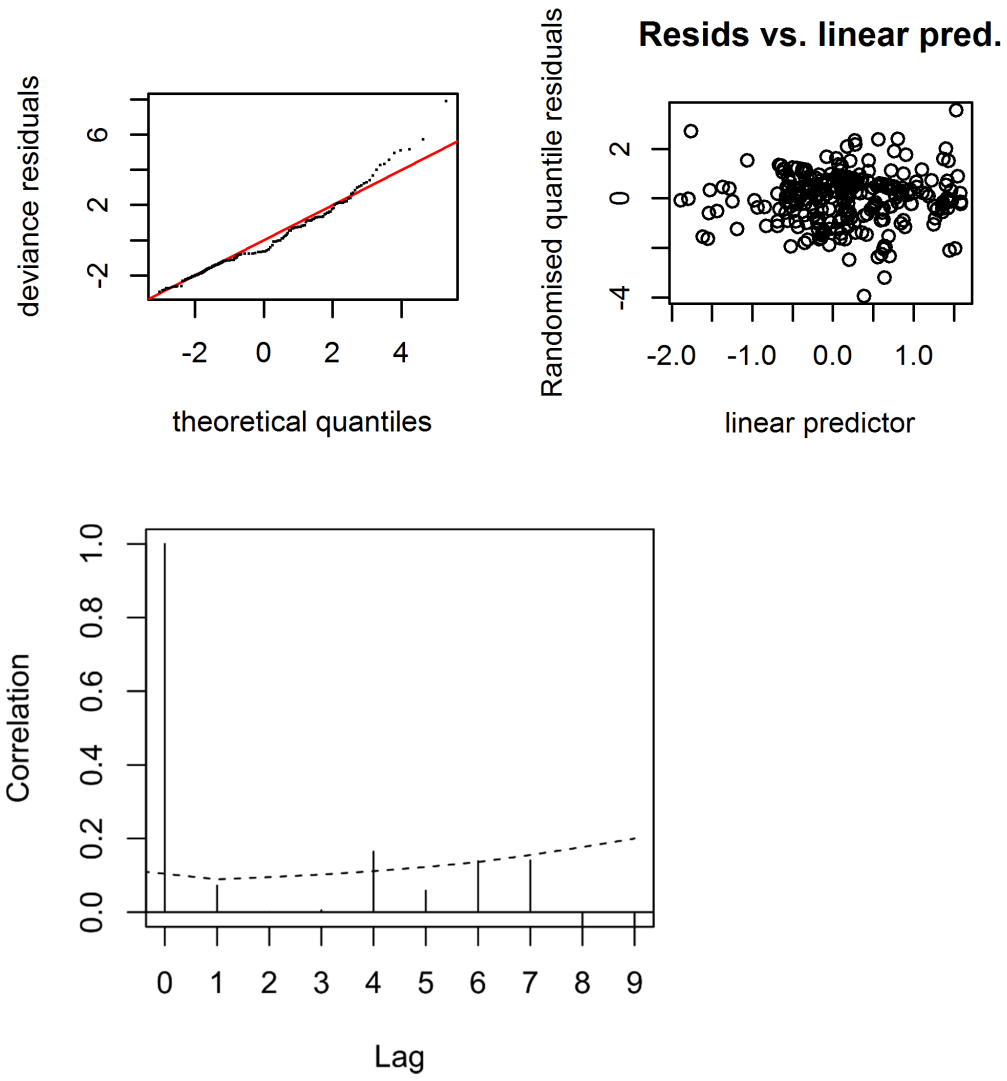

Figure S17. Normal Q–Q plot, randomised quantile residuals versus linear predictor plot, and correlogram for the Weddell seal density surface model with the lowest AIC (Table S8.1). The correlogram showed weak autocorrelation (r = 0.07 at a lag of 1 segment) in the model residuals.

Supplement 10

Figure S18. *Change in model predicted pack ice seal abundance with different levels of availability*

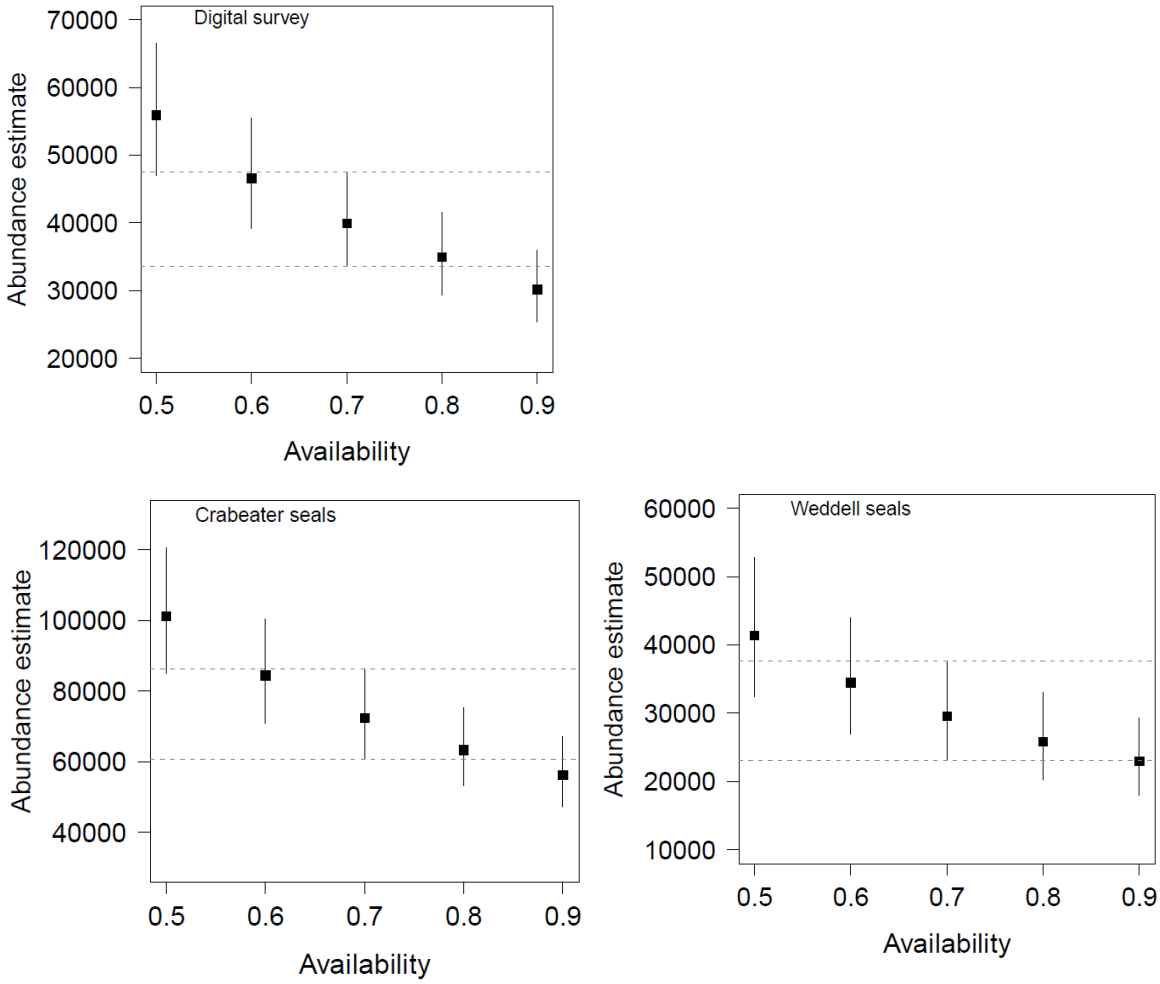

Figure S18. Our analysis assumed that 70 % of pack ice seals were available for detection during both the digital and visual surveys (availability = 0.7) (see also Supplement 2). To evaluate the sensitivity of model outputs to this haulout factor our final DSMs were refitted using availability parameters that varied from 0.5 up to 0.9. These figures show the change in predicted abundance (with 95 % confidence intervals) with changes in availability. Horizontal dotted lines indicate the upper and lower limit of the 95 % confidence interval of predicted abundance when availability equals 0.7. The mean abundance estimates for 60 % or 80 % availability was estimated within this 95 % confidence interval.

Supplement 11

Figure S19. *Model predicted pack ice seal density plotted against relative abundance of prey species sampled in ecosystem surveys*

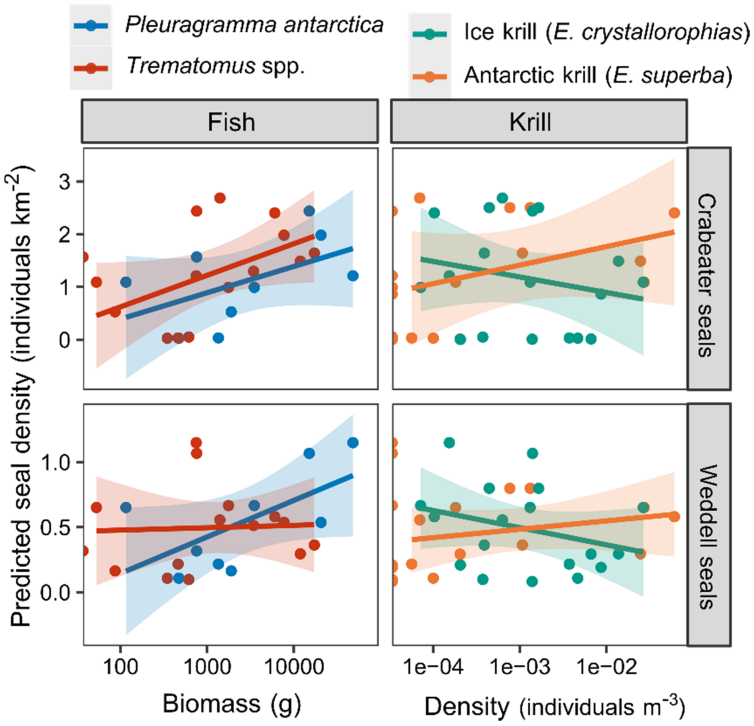

Figure S19. Density of pack ice seals (predicted by density surface models) plotted against relative abundance (on the log scale) of pack ice seal prey species (first column: notothen fish *Pleuragramma antarctica* and *Trematomus* spp.; second column: krill *E. superba* and *E. crystallorophias*) sampled in the southern Weddell Sea during January and February 2014. Seal densities were extracted from the prediction grid with %N ≥ 0 % (see main text for regressions limited to extractions from the prediction grid with %N > 10 %). Linear regressions between predicted seal densities and measures of prey abundance are indicated (shaded areas are 95 % confidence intervals).

Supplement 12

Literature cited

Bengtson JL, Laake JL, Boveng PL, Cameron MF and others (2011) Distribution, density, and abundance of pack ice seals in the Amundsen and Ross Seas, Antarctica. Deep-Sea Res II 58:1261-1276

Bouchet P, Miller D, Mannocci L, Roberts J, Harris C, Thomas L (2019) dsmextra: A toolkit for extrapolation assessments in density surface models. R package version 1.1.2

Bouchet PJ, Miller DL, Roberts JJ, Mannocci L, Harris C, Thomas L (2020) dsmextra: Extrapolation assessment tools for density surface models. Methods Ecol Evol 11: 1464–1469

Burt ML, Borchers DL, Jenkins KJ, Marques TA (2014) Using mark–recapture distance sampling methods on line transect surveys. Methods Ecol Evol 5: 1180-1191.

Conn PB, Johnson DS, Boveng PL (2015) On extrapolating past the range of observed data when making statistical predictions in ecology. PLoS ONE 10: e0141416

Derville S, Torres LG, Iovan C, Garrigue C (2018) Finding the right fit: Comparative cetacean distribution models using multiple data sources and statistical approaches. Divers Distrib 24:1657–1673

Forcada J, Trathan PN, Boveng PL, Boyd IL and others (2012) Responses of Antarctic pack ice seals to environmental change and increasing krill fishing. Biol Conserv 149:40-50

García-Barón I, Authier M, Caballero A, Vázquez JA and others (2019) Modelling the spatial abundance of a migratory predator: a call for transboundary marine protected areas. Divers Distrib 25: 346–360

Gurarie E, Bengtson JL, Bester MN, Blix AS and others (2017) Distribution, density and abundance of Antarctic ice seals off Queen Maud Land and the eastern Weddell Sea. Polar Biol 40:1149-1165

Knust R, Schröder M (2014) The expedition PS82 of the Research Vessel Polarstern to the southern Weddell Sea in 2013/14. Berichte zur Polar- und Meeresforschung 680: 1-155.

Mannocci L, Monestiez P, Spitz J, Ridoux V (2015) Extrapolating cetacean densities beyond surveyed regions: habitat-based predictions in the circumtropical belt. J Biogeogr 42:1267-1280

Michelot C, Kato A, Raclot T, Shiomi K, Goulet P, Bustamante P, Ropert-Coudert Y (2020) Sea-ice edge is more important than closer open water access for foraging Adélie penguins: evidence from two colonies. Mar Ecol Prog Ser 640:215–230

Purdon J, Shabangu FW, Yemane D, Pienaar M, Somers MJ, Findlay K (2020) Species distribution modelling of Bryde's whales, humpback whales, southern right whales, and sperm whales in the southern African region to inform their conservation in expanding economies. PeerJ 8:e9997

R Core Team. 2020. R: A language and environment for statistical computing. R Foundation for Statistical Computing, Vienna, Austria. https://www.R-project.org/.

Southwell C (2005) Optimising the timing of visual surveys of crabeater seal abundance: haulout behaviour as a consideration. Wildl Res 32:333–338

Sequeira AMM, Bouchet PJ, Yates KL, Mengersen K, Caley MJ (2018) Transferring biodiversity models for conservation: opportunities and challenges. Methods Ecol Evol 9: 1250-1264

Wege M, Salas L, LaRue M (2020) Citizen science and habitat modelling facilitates conservation planning for crabeater seals in the Weddell Sea. Diversity and Distributions 26: 1291–1304

White GC, Burnham KP (1999) Program MARK: survival estimation from populations of marked animals. Bird Study 46: S120-S139